

H. T. Banks; Nancy J. Lybeck; M. J. Gaitens; B. C. Muñoz; L. C. Yanyo
Computational methods for estimation in the modeling of nonlinear elastomers

Kybernetika, Vol. 32 (1996), No. 6, 526--542

Persistent URL: <http://dml.cz/dmlcz/125370>

Terms of use:

© Institute of Information Theory and Automation AS CR, 1996

Institute of Mathematics of the Academy of Sciences of the Czech Republic provides access to digitized documents strictly for personal use. Each copy of any part of this document must contain these *Terms of use*.



This paper has been digitized, optimized for electronic delivery and stamped with digital signature within the project *DML-CZ: The Czech Digital Mathematics Library*
<http://project.dml.cz>

COMPUTATIONAL METHODS FOR ESTIMATION IN THE MODELING OF NONLINEAR ELASTOMERS¹

H. T. BANKS, N. J. LYBECK, M. J. GAITENS, B. C. MUÑOZ AND L. C. YANYO

We report on our efforts to model nonlinear dynamics in elastomers. Our efforts include the development of computational techniques for simulation studies and for use in inverse or system identification problems. As a first step towards the full dynamic case, we present the static inverse problem, with experimental results. We also present results from the simulation of dynamic experiments.

1. INTRODUCTION

A problem of fundamental interest and great importance in modern material sciences is the development of new materials for use as both passive and active vibration suppression devices. Materials such as elastomers, rubber-like composites typically filled with inactive particles such as carbon black and silica, are frequently used in parts such as engine mounts and springs. One could imagine using active fillers, such as piezoelectric, magnetic, or conductive particles, to create a “smart” material which could be used as an active vibration suppression device. In the quest to develop such materials, accurate mathematical models of the dynamic mechanical behavior of elastomers are desirable.

The standard constitutive laws, such as Hooke’s law, were developed for metals, which behave very differently than elastomers. Thus a different approach is necessary for modeling these types of materials. There is an abundance of literature, dating back to the 1940’s, on modeling the behavior of rubber-like materials (see [12, 16, 19, 20]). Some of these models are based on the statistical molecular theory of polymers, but most are phenomenological models, utilizing strain energy functions (SEFs) and/or finite strain (FS) theories. The SEF and FS theories are, as currently used in industry, static in nature. While they can effectively capture the nonlinear behavior of elastomers, these models do not address some of the more complex behaviors exhibited by elastomers: hysteresis (the loss of potential energy); damping (the loss of kinetic energy); and the dependence of strain on environment (e. g.,

¹Research supported in part by the Air Force Office of Scientific Research under grants AFOSR F49620-93-1-0198 and F49620-95-1-0236, and the National Science Foundation under grant NSF DMS-9508617 (with matching funds for N. J. L. from Lord Corporation).

temperature), fillers (type and amount), and strain history (Mullins effect). We begin our approach as most other investigators do: with an isotropic, incompressible material under homogeneous strain. While our current efforts also do not capture many of the complex behaviors of elastomers, we can envision extensions of these models which will. These will be discussed at appropriate places.

In order to compare our partial differential equation (PDE) based method to the popular SEF methods, we must first present the general framework for the phenomenological (SEF, FS) methods. SEF material models, such as those of Mooney–Rivlin, Ogden, Treloar and numerous others, are based on strain invariants I_i , where $I_1 = \lambda_1^2 + \lambda_2^2 + \lambda_3^2$, $I_2 = \lambda_1^2\lambda_2^2 + \lambda_1^2\lambda_3^2 + \lambda_2^2\lambda_3^2$ and $I_3 = \lambda_1^2\lambda_2^2\lambda_3^2$ and the λ_i are the principal extension ratios (deformed length of unit vectors along directions parallel to the principal axes, i. e., the axes of zero shear strain). For example, the Mooney SEF is given by $U = C_1(I_1 - 3) + C_2(I_2 - 3)$, or more generally, the modified expression $U = C_1(I_1 - 3) + f(I_2 - 3)$, where f has certain qualitative properties, and is most appropriate for components where the rubber is not tightly confined and where the assumption of absolute incompressibility (implying $\lambda_1\lambda_2\lambda_3 = 1$ or $I_3 = 1$) is a reasonable approximation. The more general Rivlin SEF $U = \sum_{i+j \geq 1}^N C_{ij}(I_1 - 3)^i(I_2 - 3)^j$ and its generalization for near incompressibility (see [8]) allow higher order dependence of the SEF on the invariants.

The finite strain elastic theory due to Rivlin [16, 20] is developed with a generalized Hooke's law in an analogy to infinitesimal strain elasticity except no "small deformation" assumption is made. It includes higher order exact terms in its formulation. Moreover, finite stresses are defined relative to the *deformed* body and hence are the "true stresses" as opposed to the "nominal" or "engineering" stresses (relative to the *undeformed* body) one usually encounters in the infinitesimal linear elasticity used with metals. This Eulerian measure of strain (relative to a coordinate system convected with the deformations) – as opposed to the usual Lagrangian measure (relative to a fixed coordinate system for the undeformed body) – is an important feature of any development of models for use in analytical, computational, and experimental investigations of rubber-like material bodies. The Rivlin finite strain elasticity can be directly related to the strain energy function formulations through equations relating the finite strains \tilde{e}_{xx} , \tilde{e}_{yy} , \tilde{e}_{zz} to the extension ratios λ_1 , λ_2 , λ_3 used to define the SEF. For example, in homogeneous pure tensile strain we have $\lambda_1^2 = 1 + 2\tilde{e}_{xx}$, $\lambda_2^2 = 1 + 2\tilde{e}_{yy}$, $\lambda_3^2 = 1 + 2\tilde{e}_{zz}$ and $\tilde{e}_{yz} = \tilde{e}_{zx} = \tilde{e}_{xy} = 0$.

One can begin with a choice of the SEF or with Rivlin's finite strain formulation, and use these along with standard material independent force and moment balance derivations (the Timoshenko theory [18, 10]) as the basis of dynamic models. To illustrate this we take the simplest example: an isotropic, incompressible ($\lambda_1\lambda_2\lambda_3 = 1$) rubber-like rod under simple elongation with a finite applied stress in the principal axis direction x_1 . The finite stress theory (or the Mooney theory with SEF $U = C_1(I_1 - 3)$) leads to a true stress $\sigma = \frac{E}{3}(\lambda_1^2 - \frac{1}{\lambda_1})$ or an engineering or nominal stress for what are termed *neo-Hookean* materials

$$\sigma_{\text{eng}} = \frac{\sigma}{\lambda_1} = \frac{E}{3} \left(\lambda_1 - \frac{1}{\lambda_1^2} \right) \quad (1)$$

where in terms of deformation u in the $x_1 = x$ direction we have (since deformations

in the y and z directions are negligible)

$$\lambda_1^2 = 1 + 2\bar{\epsilon}_{xx} = 1 + 2\frac{\partial u}{\partial x} + \left(\frac{\partial u}{\partial x}\right)^2 = \left(1 + \frac{\partial u}{\partial x}\right)^2. \quad (2)$$

Here E is a generalized modulus of elasticity and we note these formulations are restricted to $\lambda_1 > -1$.

This can be used in the Timoshenko theory for longitudinal vibrations of a rubber bar to obtain (ρ = mass density, F = applied external force, A_c is the cross sectional area)

$$\rho A_c \frac{\partial^2 u}{\partial t^2} - \frac{\partial S}{\partial x} = F \quad (3)$$

where S , the internal (engineering) stress resultant, is given by

$$S = \frac{A_c E}{3} \left(\lambda_1 - \frac{1}{\lambda_1^2}\right) = \frac{A_c E}{3} \left(\frac{\partial u}{\partial x} + g\left(\frac{\partial u}{\partial x}\right)\right) \quad (4)$$

with $g(\xi) = 1 - (1 + \xi)^{-2}$. (The splitting of the stress resultant into the sum of a linear and a nonlinear term is a convention used in [2, 4], for ease of establishment of the well-posedness and convergence arguments.) This leads to the nonlinear partial differential equation

$$\rho A_c \frac{\partial^2 u}{\partial t^2} - \frac{\partial}{\partial x} \left(\frac{E A_c}{3} \frac{\partial u}{\partial x}\right) - \frac{\partial}{\partial x} \left(\frac{E A_c}{3} g\left(\frac{\partial u}{\partial x}\right)\right) = F \quad (5)$$

for dynamic longitudinal displacements of a neo-Hookean material rod in extension. Since a series expansion of g yields $g(\xi) = 2\xi - 3\xi^2 + 4\xi^3 - \dots$, this is readily seen, in the case of small displacements, to reduce to the usual longitudinal deformation equation for Hookean materials.

The neo-Hookean or simple Mooney expression for the SEF yielding the form of g in (4) has only limited practical application since it is inadequate in describing most filled elastomers. In general, one would employ equations such as (5) with a more general nonlinearity g which should be estimated from dynamic experiments. Moreover, one must also include hysteresis in the nonlinear integropartial differential equations (see [9, 12, 14, 15, 17]).

In this paper we report on our efforts to develop such a class of finite strain dynamic models to be used in design of rubber based elastomers. We develop a mathematical framework for well-posedness and approximation in the context of identification or inverse problems. Computational results as well as our use of these techniques with experiments will be discussed.

2. VARIATIONAL FORMULATION

Our immediate interest is in the design of dynamic experiments to use in determining the strain function g in models such as (5). In one type of dynamic experiments a slender rod is suspended vertically with the top end ($x = 0$) fixed, as shown in Figure 1.

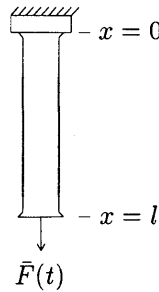


Fig. 1. Experimental setup.

Let $u(t, x)$ denote the deformation at time t of the cross section that was located at a distance x from the top when the rod was free hanging (with no applied load). Thus $u(t, 0) = 0$ for all t . The end $x = l$ of the rod is attached to a motor which supplies a force $\bar{F}(t)$ to produce some prescribed movement or deformation $u(t, l) = \Delta(t)$, $t > 0$. Hence the applied force F in (5) has the form $F(t, x) = \bar{F}(t)\delta(x - l)$ and the equation (5) and its solutions must be interpreted in some generalized or distributional sense. With the boundary conditions $u(t, 0) = 0$, $u(t, l) = \Delta(t)$ one also has initial conditions $u(0, x) = \Phi(x)$, $\dot{u}(0, x) = \Psi(x)$. In general, one should not expect the resulting initial-boundary value problem (IBVP) for (5) to have classical (smooth) solutions. For example, if we start the system from rest $\Phi \equiv 0$, $\Psi \equiv 0$ (or $\Phi \neq 0$, $\Psi = 0$ in the “preload” experiments described below) and apply a periodic force of the form $\bar{F}(t) = a \sin \omega t$, then classical solutions will not exist due to incompatibility in boundary and initial conditions. It is thus useful to write (5) in some generalized sense,

$$u_{tt} + Au + \mathcal{N}^*g(\mathcal{N}u) = F \text{ in } V^*$$

where $\mathcal{A} = A + \mathcal{N}^*g(\mathcal{N}\cdot)$ is an operator (in general, nonlinear) from a space V of functions to its dual (or conjugate dual) V^* . For the system (5), it is most convenient to choose $V = H_L^1(0, l) \equiv \{\phi \in H^1(0, l) \mid \phi(0) = 0\}$ and treat the boundary condition $u(t, 0) = 0$ as an essential boundary condition. Here $H^1(0, l)$ is the usual Sobolev space of $L_2(0, l)$ functions with derivatives in $L_2(0, l)$. If we take as pivot space $H = L_2(0, l)$ in the Gelfand triple setting $V \hookrightarrow H \hookrightarrow V^*$, then it is readily shown that the operator $\mathcal{A}u \sim \frac{\partial}{\partial x} \left(\frac{EA_c}{3} \left(\frac{\partial u}{\partial x} + g \left(\frac{\partial u}{\partial x} \right) \right) \right)$ has the form

$$(\mathcal{A}u)(\phi) = - \left\langle \frac{EA_c}{3} \frac{\partial u}{\partial x}, \phi' \right\rangle_{L_2(0,l)} - \left\langle \frac{EA_c}{3} g \left(\frac{\partial u}{\partial x} \right), \phi' \right\rangle_{L_2(0,l)}$$

as a mapping from V to V^* and reduces to the usual (and well-known) linear operator in $\mathcal{L}(V, V^*)$ in the case that the internal stress resultant (4) is linear. The corresponding weak or variational form of (5) is given by (for $F(t, x) = \bar{F}(t)\delta(x - l)$)

$$\langle \rho A_c \ddot{u}, \phi \rangle + \left\langle \frac{EA_c}{3} \frac{\partial u}{\partial x}, \phi' \right\rangle + \left\langle \frac{EA_c}{3} g \left(\frac{\partial u}{\partial x} \right), \phi' \right\rangle = \langle \bar{F}(t)\delta(x - l), \phi \rangle = \bar{F}(t)\phi(l) \quad (6)$$

for all $\phi \in V = H_L^1(0, l)$. The associated IBVP consists of finding $u(t, \cdot) \in V$ satisfying $u(t, l) = \Delta(t)$, $u(0, \cdot) = \Phi$, $\dot{u}(0, \cdot) = \Psi$. To see that this is the correct variational form, we argue as follows: Suppose u is a solution of (6) that also satisfies $u(t) \in H^2(0, l)$. Then the usual integration by parts arguments in (6) yield (assuming smoothness of g)

$$\left\langle \rho A_c \ddot{u} - \frac{\partial}{\partial x} \left(\frac{EA_c}{3} \left(\frac{\partial u}{\partial x} + g \left(\frac{\partial u}{\partial x} \right) \right) \right), \phi \right\rangle + \frac{EA_c}{3} \left(\frac{\partial u}{\partial x} + g \left(\frac{\partial u}{\partial x} \right) \right) \phi(l) = \bar{F}(t) \phi(l)$$

for all $\phi \in V = H_L^1(0, l)$. But this is equivalent to

$$\rho A_c \ddot{u} = \frac{\partial}{\partial x} \left(\frac{EA_c}{3} \left(\frac{\partial u}{\partial x} + g \left(\frac{\partial u}{\partial x} \right) \right) \right), \quad 0 < x < l \quad (7)$$

in the sense of $L_2(0, l)$ and

$$\frac{EA_c}{3} \left(\frac{\partial u}{\partial x}(l) + g \left(\frac{\partial u}{\partial x} \right)(l) \right) = \bar{F}(t), \quad t > 0. \quad (8)$$

We note that the left side of (8) is just the internal stress (see (4)) at $x = l$ which of course must match the total external force applied at the end $x = l$. (Here the "forces" are actually linear force densities – i. e., forces per unit length since ρ is mass density.)

3. STATIC MODEL

Although our ultimate goal is to use the results of dynamic experiments to determine the nonlinearity $\tilde{g}(\xi) \equiv \xi + g(\xi)$ (notice that we have combined the linear term with the nonlinear term here for the purpose of simplifying the computations), a reasonable first step is to approximate $\tilde{g}(\xi)$ using data from static pull tests. While this type of experiment cannot be used to study damping, it can be used to study the nonlinearity \tilde{g} . Given observations Δ_i representing the displacement at the end $x = l$ of the rod resulting from a constant load f_i , we can pose the static inverse problem to minimize over some admissible class $\tilde{g} \in \mathcal{G}$

$$J(\tilde{g}) = \sum_{i=1}^M |\Delta_i - u_i(l)|^2, \quad (9)$$

where u_i is the solution corresponding to \tilde{g} of a steady state version of (6)

$$\left\langle \frac{EA_c}{3} \tilde{g} \left(\frac{\partial u}{\partial x} \right), \phi' \right\rangle = f_i \phi(l). \quad (10)$$

With this goal in mind, we present first some well-posedness results for the steady state problem, and then some numerical results.

Well-Posedness of the Static Problem

In order to address the question of well-posedness for the IBVP associated with (10), we present here a nonlinear Lax–Milgram lemma for the abstract steady state equation,

$$\mathcal{A}u = f \quad \text{in } V^* \tag{11}$$

for $u \in V$, where \mathcal{A} is a nonlinear mapping from V to V^* and $V \hookrightarrow H \simeq H^* \hookrightarrow V^*$ is the usual Gelfand triple. We shall denote the H norm by $|\cdot|$, the V norm by $|\cdot|_V$ and the usual duality product by $\langle \cdot, \cdot \rangle_{V^*, V}$ where H is the pivot space. As we indicated above, we are interested in the special case in which the nonlinear mapping \mathcal{A} has the form

$$\mathcal{A} = A + \mathcal{N}^*g(\mathcal{N}\cdot) \tag{12}$$

where $A \in \mathcal{L}(V, V^*)$, $\mathcal{N} \in \mathcal{L}(V, H)$, $g : H \rightarrow H$. Here A is associated in the usual way with a sesquilinear form $\sigma : V \times V \rightarrow \mathbb{C}$ in that

$$\sigma(\phi, \psi) = \langle A\phi, \psi \rangle_{V^*, V} \quad \phi, \psi \in V.$$

We assume that σ satisfies the following conditions.

(A1) The form σ is Hermitian (symmetric) on $V \times V$.

(A2) The form σ is V -continuous, i. e., for some $c_1 > 0$

$$|\sigma(\phi, \psi)| \leq c_1 |\phi|_V |\psi|_V$$

for all $\phi, \psi \in V$.

(A3) The form σ is strictly V -elliptic, i. e., for some $k_1 > 0$

$$\sigma(\phi, \phi) \geq k_1 |\phi|_V^2$$

for all $\phi \in V$.

The linear operator \mathcal{N} in the nonlinear term is assumed to satisfy

(N1) $\mathcal{N} \in \mathcal{L}(V, H)$ and there exists $k > 0$ such that $|\mathcal{N}\phi|_H \leq \sqrt{k} |\phi|_V$ for $\phi \in V$.

The nonlinear mapping g satisfies

(N2) $g : H \rightarrow H$ is continuous and $|g(\phi)| \leq C_1 |\phi| + C_2$ for $\phi \in H$ where C_1, C_2 are nonnegative constants;

(N3) $g(0) = 0$ and for some $\epsilon < 1$ we have for all $\phi, \psi \in H$

$$\langle g(\phi) - g(\psi), \phi - \psi \rangle \geq -\epsilon k_1 k^{-1} |\phi - \psi|^2,$$

where the constants $k_1, k > 0$ are those in assumptions (A3) and (N1), respectively.

The conditions (A1)–(A3) are quite standard in the theory of linear systems while the conditions (N1)–(N3) are readily shown to hold for classes of the elastomer models discussed in Section 1. Under these assumptions, one can prove existence of unique solutions to (11) which can be viewed as a nonlinear version of the generalized Lax–Milgram lemma ([21] and [11]). The proof of Lemma 2.1, which can be found in [4], is constructive, and can be used to show convergence of certain Galerkin approximations. These results can also be considered a corollary of earlier results due to Minty and Browder ([13, 7]).

Lemma 2.1. Under (A1)–(A3), (N1)–(N3), equation (11) has a unique solution u in V for each $f \in V^*$.

Numerical Results for the Static Inverse Problem

We now proceed to the numerical estimation of \tilde{g} . Since methods currently exist to estimate an SEF from static testing results, we have a basis for comparison of our methods with commonly accepted techniques. The simplest such experiment is the static pull test, in which a slender rod is suspended vertically with the top end ($x = 0$) fixed, as shown above in Figure 1. Let $u_i(x)$ denote the deformation (under a constant load f_i) of the cross section that was located at a distance x from the top when the rod was free hanging (with no applied load). Thus $u_i(0) = 0$, and the end $x = l$ of the rod is subjected to a constant force f_i . The sample satisfies the steady state equation

$$\begin{aligned} \frac{\partial}{\partial x} \left(A_c \hat{g} \left(\frac{\partial u_i}{\partial x} \right) \right) &= 0 \quad 0 < x < l \\ A_c \hat{g} \left(\frac{\partial u_i}{\partial x} \right) (l) &= f_i \\ u_i(0) &= 0 \\ u_i(l) &= \Delta_i \end{aligned} \tag{13}$$

where the nonlinearity $\hat{g} = \frac{E}{3} \tilde{g}$ is unknown. We seek to find \hat{g} minimizing

$$J(\hat{g}) = \sum_{i=1}^k |\Delta_i - u_i(l; \hat{g})|^2 \tag{14}$$

over some class of admissible functions $\hat{g} \in \mathcal{G}$, where $\{\Delta_i, f_i\}_{i=1}^k$ are data from a series of “static pull” experiments.

In general, problems such as those involving (14) are infinite dimensional in both state and parameter space and hence, for computational purposes, finite dimensional approximations must be made. For state approximation, one typically uses Galerkin techniques. However, in the case that \hat{g} is monotone, the system of equations (13) satisfied by the rod can be simplified to

$$u_i(l) = \int_0^l \hat{g}^{-1} \left(\frac{f_i}{A_c} \right) dx, \tag{15}$$

and thus one may avoid making a state approximation. For parameter space discretization (i. e., approximation of \hat{g}), one may use a finite dimensional parameterization or representation. In light of (15), it is appropriate to approximate \hat{g}^{-1} using M approximating piecewise linear elements (e. g., linear splines)

$$\hat{g}_M^{-1}(x) = \sum_{j=1}^M c_j \eta_j(x).$$

The least squares spline inverse problem (LSSIP) is then equivalent to: find $\vec{c} \in \mathbb{R}^M$ minimizing

$$J(\vec{c}) = \sum_{i=1}^k |\Delta_i - u_i(l; \vec{c})|^2. \tag{16}$$

(Since we expect \hat{g} to be monotone, estimating the inverse function is an acceptable technique.) We have used our methods (with 15 linear splines parameterizing \hat{g}^{-1}) to fit the data from static tensile strain experiments. One of the standard engineering techniques is to use data to estimate a cubic Mooney–Rivlin SEF (see [19], [20]). As seen in [20], the engineering stress in the x direction which arises from the estimated SEF U is given by the equation

$$\sigma_{\text{eng}} = 2 \left(\lambda_1 - \frac{1}{\lambda_1^2} \right) \left\{ \frac{\partial U}{\partial I_1} - \frac{1}{\lambda_1} \frac{\partial U}{\partial I_2} \right\}.$$

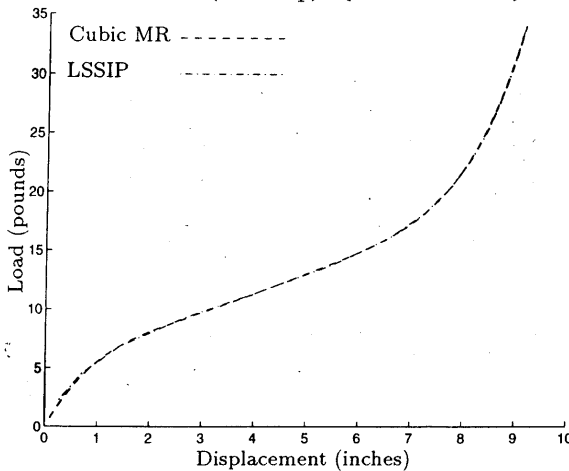


Fig. 2. Load vs. displacement for static pull experiment.

Figure 2 demonstrates that the results from the two methods, viewed in the load-deflection plane, are nearly identical. The material used for the sample is a common elastomer formulation, similar to those used for tire sidewalls. It is a blend of natural rubber (cis-polyisoprene) and polybutadiene. It includes approximately 30 percent carbon black by weight, and is crosslinked with sulfur and accelerators. The data

is not included on the graph in Figure 2, as both fits are so close that the curves would be indistinguishable.

A common practice is to view the results in the reduced stress plane (see [19], pp. 95–99, [20], pp. 51–52), instead of the load-deflection plane. For a rod in uniaxial tension, the reduced stress (or Mooney stress) is given by

$$\sigma_M = \frac{\sigma_{\text{eng}}}{2(\lambda_1 - \lambda_1^{-2})} = \frac{\partial U}{\partial I_1} - \frac{1}{\lambda_1} \frac{\partial U}{\partial I_2}.$$

The reduced stress σ_M is then plotted as a function of $1/\lambda_1$. Historically, this was used to gain some insight into the dependence of the SEF U on I_1 and on I_2 . As seen in Figure 3, the reduced stress curve generated from our method approximates the curve generated from the data more closely than does the curve resulting from the standard SEF method. Thus the approach proposed in this note offers the potential for improvement on existing industrial methods.

4. DYNAMIC MODEL

In the dynamic experiments being discussed here, the system will be preloaded, i. e., we take the initial state of the rod so that $u(0, l) = \Delta$ (and thus the initial displacement Φ is taken as the solution of the steady state version of (7) subject to $u(0) = 0$, $u(l) = \Delta$). Then we take $\Delta(t) = \Delta + d(t)$ where $d(t) > -\Delta$ is some prescribed dynamics for the end $x = l$. In this way one can guarantee that the rod remains in simple extension, and compression (which leads to nontrivial shear) is not present during the course of the experiments.

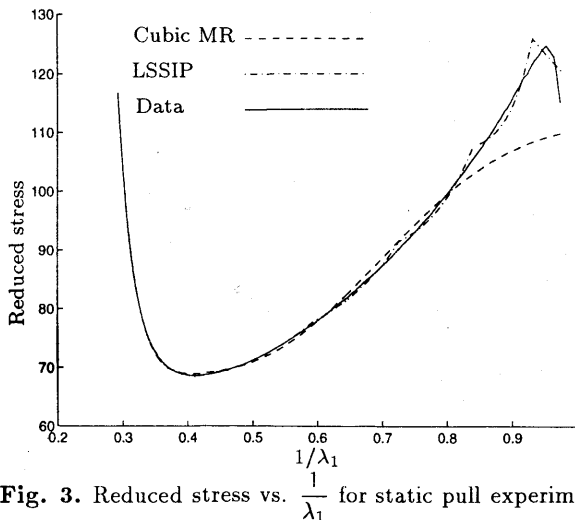


Fig. 3. Reduced stress vs. $\frac{1}{\lambda_1}$ for static pull experiment.

To determine the nonlinearity $\tilde{g}(\xi)$, one has, for a given input $\Delta(t)$ (or $\bar{F}(t)$), observations z_i which are proportional to the strain $\frac{\partial u}{\partial x}(t_i, 0)$ at the fixed end. The

estimation problem of interest consists of minimizing over some admissible class $\tilde{g} \in \mathcal{G}$

$$J(\tilde{g}) = \sum_{i=1}^M \left| z_i - \mu \frac{\partial u}{\partial x}(t_i, 0; \tilde{g}) \right|^2 \tag{17}$$

where u is the solution of (6) corresponding to \tilde{g} . One may also be fortunate enough to have observations \hat{u}_i of deformations $u(t_i, \bar{x}; \tilde{g})$ at some point $x = \bar{x}$, $0 < \bar{x} < l$, and then the optimization criterion (17) can be modified accordingly.

Well-Posedness of the Dynamic Problem

Returning to the question of well-posedness for the IBVP associated with (6), in the event sufficient damping is present (the equations (5) or (6) are undamped and hence are not realistic physically), one may use the techniques and results of [1], [2] to establish well-posedness for a rather generous class of nonlinearities, even though we only have $F(t, \cdot)$ in V^* for the problems at hand. (For g linear, well-posedness follows immediately from the results in [3].) Under appropriate assumptions on the damping sesquilinear form and the additional assumptions that g is of gradient type (i.e., there exists $G : H \rightarrow \mathbb{R}^1$ with the Frechet derivative of G given by $G'(\phi)\psi = \text{Re}(g(\phi), \psi)$ for $\psi \in H$), and for any $\phi \in H$ the Frechet derivative $g'(\phi)$ exists and satisfies $g'(\phi) \in \mathcal{L}(H)$ with $|g'(\phi)|_{\mathcal{L}(H)} \leq C_3$ for some constant C_3 independent of ϕ , one can use (A1)–(A3) and (N1)–(N3) to establish existence, uniqueness and certain regularity for solutions of (5). Details are given in [2].

Numerical Approximations

The ultimate goal of solving an inverse problem to determine the nonlinearity g must be considered when developing a numerical scheme to solve the forward problem (6). The presence of the prescribed deformation $u(t, l) = \Delta + d(t)$ indicates that a Tau-Galerkin method would be a convenient method for solving the weak formulation (6). The theory developed in [6] further suggests that a Tau-Galerkin method is an appropriate choice in the context of solving least-squares parameter estimation problems.

For a given g we use a Tau-Galerkin method with linear splines for the spatial discretization, and a Fehlberg fourth-fifth order Runge-Kutta method in time. We therefore seek an approximate solution to (6) of the form

$$u^N(t, x) = \sum_{j=1}^N w_j(t) L_j(x)$$

where the L_j are linear splines (given below), and w_j are unknown functions of time. In the Tau method, we impose the boundary condition $u(t, l) = \Delta + d(t)$ on the trial solutions u^N , not on the individual basis elements. The boundary condition $u(t, 0) = 0$ is treated as an essential boundary condition and is imposed directly on each of the basis elements L_j .

Let $h = \frac{l}{N}$ denote the grid spacing. Let $x_j = jh$, $j = 1, \dots, N$ be the grid points. The usual linear splines are defined for $1 \leq j \leq N-1$ by

$$L_j(x) = \begin{cases} 0, & 0 \leq x \leq (j-1)h \\ x/h - (j-1), & (j-1)h \leq x \leq jh \\ -x/h + j + 1, & jh \leq x \leq (j+1)h \\ 0, & x \geq (j+1)h \end{cases}$$

with

$$L_N(x) = \begin{cases} 0, & 0 \leq x \leq (N-1)h \\ x/h - N + 1, & x \geq (N-1)h. \end{cases}$$

In order to use the Runge-Kutta method, (6) must be written as a first order system in time. To accomplish this, we rewrite the weak formulation (6) as

$$\dot{u}_1 = u_2 \tag{18}$$

and for each $\phi \in H_0^1(0, l) \subsetneq V \equiv H_L^1(0, l)$

$$\int_0^l \dot{u}_2 \rho A_c \phi \, dx = - \int_0^l \phi' \frac{A_c E}{3} \tilde{g} \left(\frac{\partial u_1}{\partial x} \right) \, dx. \tag{19}$$

The approximate solutions of (18) and (19) are given by

$$u_1^N(t, x) = \sum_{j=1}^{N-1} w_j(t) L_j(x) + (\Delta + d(t)) L_N(x),$$

and

$$u_2^N(t, x) = \sum_{j=1}^{N-1} \psi_j(t) L_j(x) + \dot{d}(t) L_N(x).$$

Substituting the approximate solutions into (18) we obtain equations

$$\dot{w}_j(t) = \psi_j(t), \quad j = 1, \dots, N-1.$$

Substituting the approximate solutions into (19), and choosing $\phi = L_k$, we find

$$\begin{aligned} & \int_0^l \left(\sum_{j=1}^{N-1} \dot{\psi}_j L_j + \ddot{d} L_N \right) \rho A_c L_k \, dx \\ &= - \int_0^l L_k' \frac{A_c E}{3} \tilde{g} \left(\sum_{j=1}^{N-1} w_j L_j' + (\Delta + d) L_N' \right) \, dx. \end{aligned}$$

For fixed t the discrete system is achieved by allowing k to vary between 1 and $N - 1$. The following notation is necessary to write down the discrete system. Define the (symmetric) tridiagonal mass matrix M with entries

$$[M_{i,i}] = \int_0^l \rho A_c L_i^2 dx,$$

and

$$[M_{i,i+1}] = [M_{i+1,i}] = \int_0^l \rho A_c L_i L_{i+1} dx.$$

Define the vector \vec{G} with entries

$$\vec{G}_i = - \int_0^l L_i' \frac{A_c E}{3} \tilde{g} \left(\sum_{j=1}^{N-1} w_j L_j' + (\Delta + d) L_N' \right) dx \quad i = 1, \dots, N - 2,$$

and

$$\vec{G}_{N-1} = - \int_0^l L_{N-1}' \frac{A_c E}{3} \tilde{g} \left(\sum_{j=1}^{N-1} w_j L_j' + (\Delta + d) L_N' \right) - \ddot{d} \rho A_c L_N L_{N-1} dx.$$

The first order discrete system is then given by

$$\begin{bmatrix} I & 0 \\ 0 & M \end{bmatrix} \begin{bmatrix} \vec{w} \\ \vec{\psi} \end{bmatrix} = \begin{bmatrix} 0 & I \\ 0 & 0 \end{bmatrix} \begin{bmatrix} \vec{w} \\ \vec{\psi} \end{bmatrix} + \begin{bmatrix} \vec{0} \\ \vec{G}(\vec{\psi}) \end{bmatrix},$$

$$\begin{bmatrix} \vec{w}(0) \\ \vec{\psi}(0) \end{bmatrix} = \begin{bmatrix} \vec{\Phi} \\ \vec{\Psi} \end{bmatrix}.$$

Numerical Studies

We have used the numerical scheme outlined above in numerical simulation studies to aid in design of experiments. We describe briefly here some of our findings.

The first question to be addressed in using the approximation schemes is related to their accuracy. One can prove convergence results: as $N \rightarrow \infty$, the approximate solutions u^N converge to the solution u of (6). However, this does not answer the question of the value of N that we fix to use in our calculations. To aid in this matter, we performed a series of eigenvalue calculations with the approximate system in the case of a Hookean material ($g(\xi) = 2\xi$ in (5)). For a rod of length $l = 15$ cm, and constant cross section, one finds that the eigenvalues are given by $\lambda_n = n\pi/l\sqrt{E/\rho}$. Choosing material parameters $E = 2.1 \times 10^7$ dyn/cm², $\rho = 0.92$ g/cm³, we obtain the corresponding natural frequencies $f_n = \lambda_n/(2\pi)$ given by $f_n = 159.25n$. Eigenvalue calculations with the approximate systems demonstrated good approximation of the first eight natural frequencies at $N = 64$. For example, at $N = 48$ and 64 we obtained $f_1^{48} = 159.28$, $f_1^{64} = 159.27$ to approximate $f_1 = 159.25$ while $f_7^{48} = 1124.55$, $f_7^{64} = 1120.28$ approximate $f_7 = 1114.75$. Similar approximates are found

for the other frequencies. Based on these eigenvalue studies for the linear systems (of course, the ideas of eigenvalues and modes are not useful for the neo-Hookean system) we used $N = 48$ in our calculations, including those reported on here.

We considered a number of questions in support of our experimental design goals and we list several of these. (i) What shape ($l, A_c = A(x)$, etc.) should be used in order to provide ample information about the material and yet will be easily constructed? (ii) If additional observations (say of displacement) are possible, where should these be taken to maximize the differences between Hookean and neo-Hookean material responses? (We know, for example, that displacement sensors near nodal points for a linear system is not an intelligent choice!) (iii) What type of input signals will sufficiently distinguish the Hookean and neo-Hookean responses so as to enhance our possibilities for identifying g from vibration response data? (iv) How should we test damping? The linear version of equation (6) is undamped (does the nonlinearity g itself provide some type of damping or dissipation of input energy?), while the experimental responses will definitely exhibit significant damping.

We discuss briefly some of our findings related to two of these questions. First the question of damping is a difficult one that we are still pursuing. However, as the graphs in Figure 4 reveal, the Hookean model, as expected, has no inherent damping. Each graph in Figure 4 corresponds to a simulation with zero initial displacement but with the same nonzero initial velocity (this simulates a structure that has been excited with the same energy input at $t = 0$ and afterwards allowed to freely oscillate). The neo-Hookean response suggests that there is some inherent energy reduction in the nonlinear system but it clearly is not damping in the traditional sense we understand. It also does not correspond to the rapid dissipation we see in oscillating rubber samples. The displacement is shown at $l/4$ in anticipation of using FFT's to study the natural frequencies excited (when measured at l/k , $k = 1, 2, \dots$, information on the k th mode is lost).

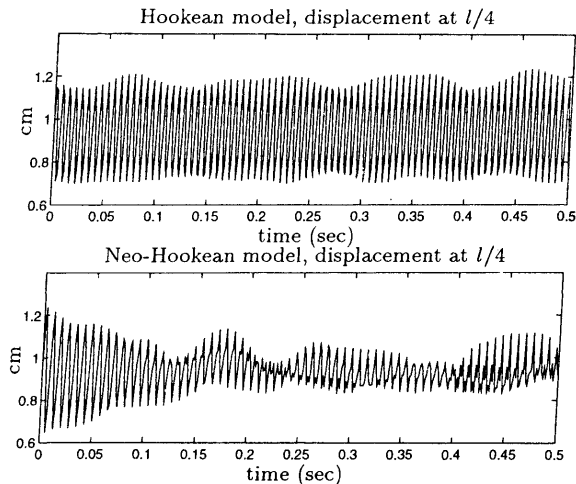


Fig. 4. Damping experiment for both a Hookean and a neo-Hookean model.

The question of type of input signal to use has yielded quite nicely to our numer-

ical investigations. We have considered persistent sinusoidal inputs $d(t) = a \sin \omega t$ with the driving frequency of $f = \omega/(2\pi)$ near and far from resonance for the linear system. We also considered periodic triangular inputs (a “sawtoothed” sinusoidal that is between a square wave and a smooth sinusoidal). In many numerical experiments, it was observed that the driving frequency dominated the responses with varying levels of energy exciting the natural structural modes of the Hookean system. In FFT’s of the neo-Hookean responses, one sees energy concentrations but, as one might expect, not so sharply as in systems with modes.

One important constraint on the periodic input signals is the frequency range for f possible in the experimental test equipment. While a frequency sweep (say between 0 and 500 Hz) would reveal significant information, we are physically restricted (at least in the range of deformations we are interested in) to excitations in the 0–25 Hz range. These (in the range of displacements allowed) do not yield really substantial excitation in frequencies much beyond the first natural frequency of the Hookean model.

Our most promising results to date suggest that a simulated “impulse” for the system might sufficiently distinguish the Hookean and neo-Hookean responses when working in the frequency/displacement ranges dictated by our experimental equipment. In Figures 5 and 6 we plot the input signal (a triangular displacement approximating an impulse input) and the FFT of the corresponding displacement at $x = l/4$ in the rod for an input possible with frequency set at 15 Hz. Figure 5 contains the Hookean response while Figure 6 is the neo-Hookean. In Figures 7 and 8 we give similar plots for an input signal corresponding to $f = 25$ Hz.

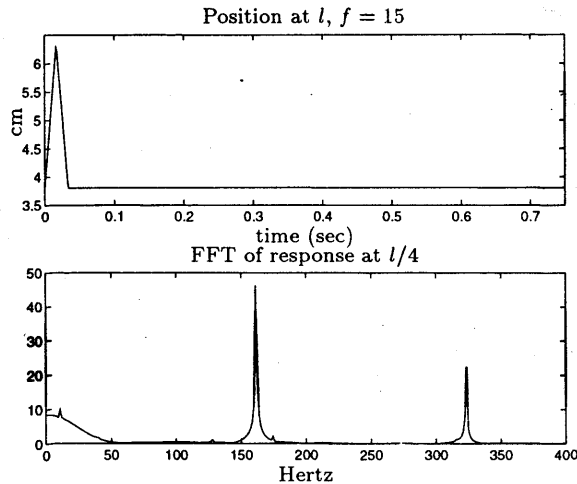


Fig. 5. Hookean response at 15 Hz.

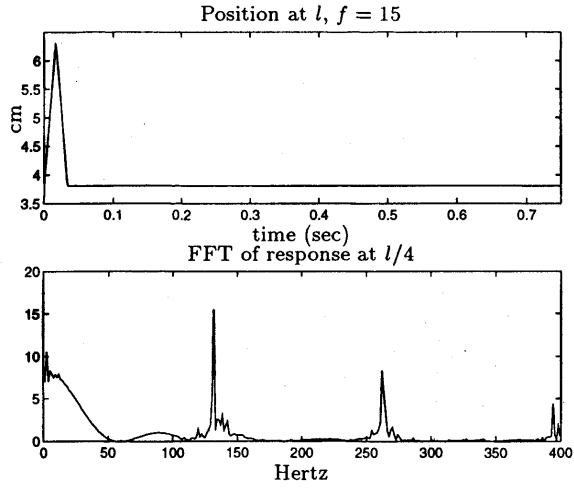


Fig. 6. Neo-Hookean response at 15 Hz.

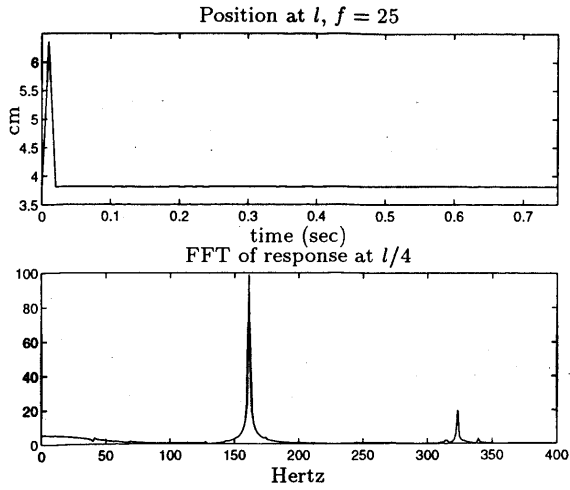


Fig. 7. Hookean response at 25 Hz.

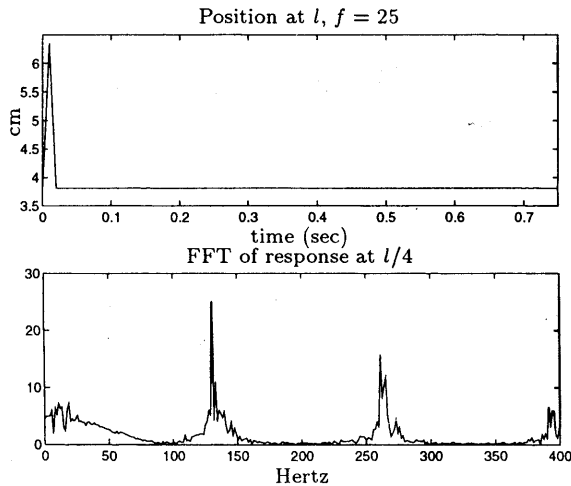


Fig. 8. Neo-Hookean response at 25 Hz.

5. CONCLUDING REMARKS

In the discussions above we have outlined some of our initial efforts on the intellectually stimulating but difficult problems related to the understanding of the dynamics of filled elastomers. We are currently conducting experiments and developing computational techniques for the estimation of g in (6) from vibration response data. Moreover, in related studies [5] we are developing models and computational schemes to treat hysteresis as well as damping in composite material structures containing viscoelastic components.

(Received February 14, 1996.)

REFERENCES

- [1] H. T. Banks, D. S. Gilliam and V. I. Shubov: Well-Posedness for a One Dimensional Nonlinear Beam. Technical Report No. CRSC-TR94-18, NCSU, 1994; *Computation and Control IV*, K. Bowers and J. Lund, eds., Birkhäuser, Boston 1995, pp. 1-21.
- [2] H. T. Banks, D. S. Gilliam and V. I. Shubov: Global Solvability for Damped Abstract Nonlinear Hyperbolic Systems. Technical Report No. CRSC-TR95-25, NCSU, 1995; *Differential and Integral Equations*, to appear.
- [3] H. T. Banks, K. Ito and Y. Wang: Well Posedness for Damped Second Order Systems with Unbounded Input Operators. Technical Report No. CRSC-TR93-10, NCSU, 1993; *Differential and Integral Equations* 8 (1995), 587-606.
- [4] H. T. Banks and N. J. Lybeck: A Nonlinear Lax-Milgram Lemma Arising in the Modeling of Elastomers. Technical Report No. CRSC-TR95-37, NCSU, 1995; *Nonlinear Partial Differential Equations*, Collège de France Seminar, Vol. 13, 1996, to appear.

- [5] H. T. Banks, N. Medhin and Y. Zhang: A Mathematical Framework for Curved Active Constrained Layer Structures: Well-posedness and Approximation. Technical Report No. CRSC-TR95-32, NCSU, 1995; Numer. Funct. Anal. Optim., to appear.
- [6] H. T. Banks and J. G. Wade: Weak Tau approximations for distributed parameter systems in inverse problems. Numer. Funct. Anal. Optim. 12 (1991), 1-31.
- [7] F. E. Browder: Nonlinear monotone operators and convex sets in Banach spaces. Bull. Amer. Math. Soc. 71 (1965), 780-785.
- [8] D. J. Charlton, J. Yang and K. K. Teh: A review of methods to characterize rubber elastic behavior for use in finite element analysis. Rubber Chemistry & Technology 67 (1994), 481-503.
- [9] R. M. Christensen: Theory of Viscoelasticity. Academic Press, New York 1982.
- [10] R. W. Clough and J. Penzien: Dynamics of Structures. McGraw-Hill, New York 1975.
- [11] R. Dautray and J. L. Lions: Mathematical Analysis and Numerical Methods for Science and Technology. Vol. 2: Functional and Variational Methods. Springer-Verlag, Berlin - Heidelberg 1988.
- [12] J. D. Ferry: Viscoelastic Properties of Polymers. John Wiley & Sons, New York 1980.
- [13] G. J. Minty: Monotone (nonlinear) operators in Hilbert space. Duke Math. J. 29 (1962), 341-346.
- [14] A. C. Pipkin: Lectures on Viscoelasticity Theory. Springer-Verlag, Berlin - Heidelberg 1972.
- [15] M. Renardy, W. J. Hrusa and J. A. Nohel: Mathematical Problems in Viscoelasticity. Pittman Monograph, Longman/J. Wiley & Sons, 1987.
- [16] R. S. Rivlin: Large elastic deformations of isotropic materials I, II, III. Philos. Trans. Roy. Soc. London Ser. A 240 (1948), 459-490, 491-508, 509-525.
- [17] I. H. Shames and F. A. Cozzarelli: Elastic and Inelastic Stress Analysis. Prentice Hall, Englewood Cliffs, N. J. 1992.
- [18] S. Timoshenko, D. H. Young and W. Weaver, Jr.: Vibration Problems in Engineering. J. Wiley & Sons, New York 1974.
- [19] L. R. G. Treloar: The Physics of Rubber Elasticity. Third edition. Clarendon Press, Oxford 1975.
- [20] I. M. Ward: Mechanical Properties of Solid Polymers. Second Edition. John Wiley & Sons, New York 1983.
- [21] J. Wloka: Partial Differential Equations. Cambridge University Press, Cambridge 1987.

Dr. H. T. Banks and Dr. N. J. Lybeck, Center for Research in Scientific Computation, Department of Mathematics, North Carolina State University, Raleigh, NC 27695. U. S. A.

Mr. M. J. Gaitens, Dr. B. C. Muñoz and Dr. L. C. Yanyo, Lord Corporation, Thomas Lord Research Center, 405 Gregson Drive, Cary, NC 27511. U. S. A.